Journal of Nuclear Materials 393 (2009) 87–91

Contents lists available at ScienceDirect

Journal of Nuclear Materials

journal homepage: www.elsevier.com/locate/jnucmat

Structural study of $Pu_{1-x}Am_xO_2$ (x = 0.2; 0.5; 0.8) obtained by oxalate co-conversion

A. Jankowiak [a,*], C. Maillard [b], L. Donnet [c]

[a] Commissariat à l'Energie Atomique (CEA), CEA/DEN/DTEC/SDTC/LEMA, 30207 Bagnols-sur-Cèze cedex, France
[b] Commissariat à l'Energie Atomique (CEA), CEA/DEN/DRCP/SE2A/LEHA, 30207 Bagnols-sur-Cèze cedex, France
[c] Commissariat à l'Energie Atomique (CEA), CEA/DEN/DTEC/SDTC/DIR, 30207 Bagnols-sur-Cèze cedex, France

ARTICLE INFO

Article history:
Received 1 April 2009
Accepted 18 May 2009

ABSTRACT

This study describes the synthesis and the characterisation of $Pu_{1-x}Am_xO_2$ (x = 0.2; 0.5; 0.8) mixed oxides obtained by oxalate co-conversion. We studied the self-irradiation effect in these compounds at the structural scale. We determined, for each composition, the initial lattice parameter and the equation describing its variation versus time and displacements per atom. Similarly to other α emitting compounds, it was observed a fast lattice parameter expansion rate, followed by a stabilisation at a maximum value. The observations also showed that the initial expansion rate varies according to the Am content and the maximum value to the Pu content. However, for all compositions, the lattice parameter relative variations are the same.

1. Introduction

The EUROTRANS project investigates the transmutation of transuranium elements in dedicated reactors (ADS, FNR). The study includes various subject areas such as: neutronics, physical properties, coolant type and experimental work concerning the fabrication of minor actinides compounds for irradiation experiments and thermo-physical properties determination.

For this program, the CEA was in charge of the synthesis of three $Pu_{1-x}Am_xO_2$ (x = 0.2; 0.5; 0.8) mixed oxides by oxalate co-conversion. Although $Pu_{1-x}Am_xO_2$ have probably a crystalline structure and self-irradiation behaviour similar to PuO_2 and AmO_2, the data concerning this type of materials are missing in the literature. It was considered as interesting to perform a structural study to determine, for each composition, the initial lattice parameter and the equation describing its variation versus time and displacements per atom.

2. Experimental

2.1. $Pu_{1-x}Am_xO_2$ synthesis

$Pu_{1-x}Am_xO_2$ mixed oxides were obtained by oxalate co-conversion technique which provides very fine and high purity powder if it is compared to a conventional high temperature solid state reaction. This technique includes two steps:

– Precipitation in acidic medium (1):

$$\left(Am^{3+}\right)_{x_1} + \left(Pu^{4+}\right)_{x_2} + \frac{3x_1+4x_2}{2}C_2O_4^{2-} \rightarrow Am_{x_1}Pu_{x_2}(C_2O_4)\frac{3x_1+4x_2}{2}, nH_2O. \quad (1)$$

– Calcination in air (2):

$$Am_{x_1}Pu_{x_2}(C_2O_4)\frac{3x_1+4x_2}{2} + O_2 \rightarrow (Am_{x_1}Pu_{x_2})O_2 + (3x_1+4x_2)CO_2. \quad (2)$$

Isotopic compositions of Pu and Am as well as the results of the chemical analysis performed on the starting solutions are given in Table 1. It was found that the elemental content in each composition was in good agreement with the aimed compositions.

3. Results and discussion

3.1. Particle size and specific surface areas determination

The particle size distributions were obtained using a Coulter Multisizer II. The powder was added to a saturated Isoton solution.

The specific surface areas were determined by the BET method using a Coulter SA 3100 analyzer. The results are reported in Table 2. It can be seen that the values are within the order of magnitude for this type of powder (eg: AmO_2, PuO_2).

3.2. SEM

The powder morphology was studied by scanning electron microscopy with a Jeol T-200. Fig. 1(a), (b) and (c) shows the

* Corresponding author. Tel.: +33 4 66 79 65 42; fax: +33 4 66 79 16 49.
E-mail address: aurelien.jankowiak@cea.fr (A. Jankowiak).

0022-3115/$ - see front matter © 2009 Elsevier B.V. All rights reserved.
doi:10.1016/j.jnucmat.2009.05.009

Table 1
Isotopic compositions of Pu and Am and $Pu_{1-x}Am_xO_2$ chemical analysis.

Pu isotopic composition					
Isotope	^{238}Pu	^{239}Pu	^{240}Pu	^{241}Pu	^{242}Pu
Atom%	0.18 ± 0.02	75.61 ± 0.03	21.00 ± 0.02	2.53 ± 0.01	0.68 ± 0.01
Am isotopic composition					
Isotope	^{241}Am		^{242}Am	^{243}Am	
Atom%	100.000 ± 0.005		<0.001	<0.001	
$Pu_{1-x}Am_xO_2$ chemical analysis					
Compound	$Pu_{0.80}Am_{0.20}O_2$		$Pu_{0.50}Am_{0.50}O_2$	$Pu_{0.20}Am_{0.80}O_2$	
Measured composition	$Pu_{0.79}Am_{0.21}O_2$		$Pu_{0.51}Am_{0.49}O_2$	$Pu_{0.20}Am_{0.80}O_2$	

Table 2
$Pu_{1-x}Am_xO_2$ powder characteristics.

Compound	$Pu_{0.80}Am_{0.20}O_2$	$Pu_{0.50}Am_{0.50}O_2$	$Pu_{0.20}Am_{0.80}O_2$
Specific surface area ($m^2\,g^{-1}$)	5.6	5.7	2.0
Mean particle size (μm)	3.8 ± 0.5	3.7 ± 0.4	2.3 ± 1.2

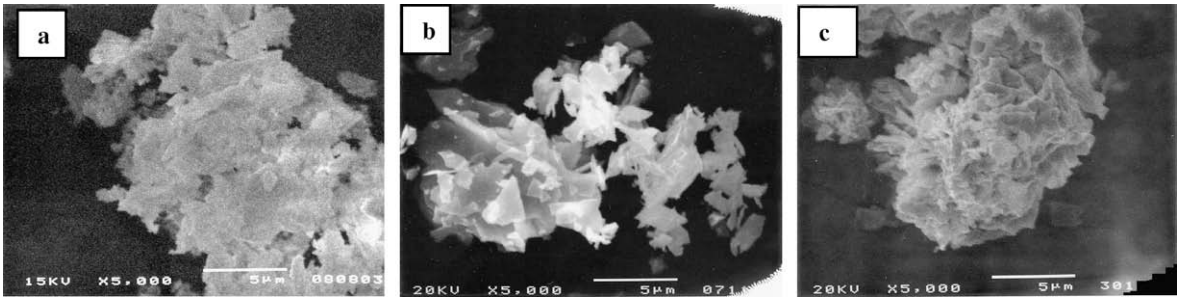

Fig. 1. SEM powder morphology: (a) $Pu_{0.79}Am_{0.21}O_2$, (b) $Pu_{0.51}Am_{0.49}O_2$, (c) $Pu_{0.20}Am_{0.80}O_2$.

SEM images of the three compounds particles. As expected, this wet-chemical route leads to very fine particles.

3.3. XRD

3.3.1. Structural study

XRD experiments were performed on a Bruker D8 Advance using a molybdenum anticathode in the range 8–55° at 1.6°/h. The computation programs used for the lattice parameter refinement and phase determination were EVA and TOPAS. For each experiment, gold powder was added to the sample as an internal standard.

As indicated in Fig. 2, XRD patterns of the three $Pu_{1-x}Am_xO_2$ were obtained as close as possible to the synthesis in order to reduce the self-irradiation impact. The corresponding peak positions and intensities are reported in Table 3.

In Fig. 3, it can be seen that $Pu_{1-x}Am_xO_2$ have a fcc structure and exhibit single narrow peaks located between PuO_2 and AmO_2 peaks suggesting that single phased compounds were synthesized.

3.3.2. Lattice parameter variation in $Pu_{1-x}Am_xO_2$ ($x = 0.2; 0.5; 0.8$)

Self-irradiation induces structural defects and significant changes in the materials properties [1]. Lattice swelling, phase transformations, amorphisation and thermal conductivity decrease can be observed [2,3].

In our case, the high α decay rate in ^{241}Am and ^{237}Np recoil nuclei produce important damages at the structural scale. The most important part of the disorder is due to the ^{237}Np nucleus which has an energy of about 91 keV. As a consequence of the defects formation, the lattice parameter tends to expand versus time [4]. The curves describing this variation are generally expressed by (3) and (4):

$$\frac{\Delta a}{a_0} = A \cdot \left(1 - e^{-Bt}\right), \tag{3}$$

$$\frac{\Delta a}{a_0} = A \cdot \left(1 - e^{-C\lambda t}\right), \tag{4}$$

where a is the lattice parameter, a_0 the initial value of the lattice parameter, A, B and C are constant, t is the time in days and λ the radioactive constant (i.e.: 432.7y for ^{241}Am). Table 4 gives expressions found in the literature for various AmO_2 and PuO_2 studies. It can be seen that the most significant difference mainly concerns the B coefficient. This is explained by the type of studied element and especially the isotopic composition since B coefficient is related to the radioactive constant and the α decay rate.

The curve consists in a fast expansion rate of the lattice parameter at the beginning followed by a stabilisation at a maximum value [5,6]. Many articles concerning this phenomenon explain the curve shape [7–12], and [13]. It should be noted that R.B. Roof [9] studies on $^{238(80\%)}PuO_2$ lead to a curve with a maximum for t = 65 weeks and a minimum at the end of 200 weeks. It is the only example of this type of curve in the literature.

In this work, the lattice parameter of each composition has been studied for 400 days. From the experimental data in Fig. 4, we determined initial and maximum values of the lattice parameter and expressions describing its variations versus time. The results are reported in Tables 5 and 6.

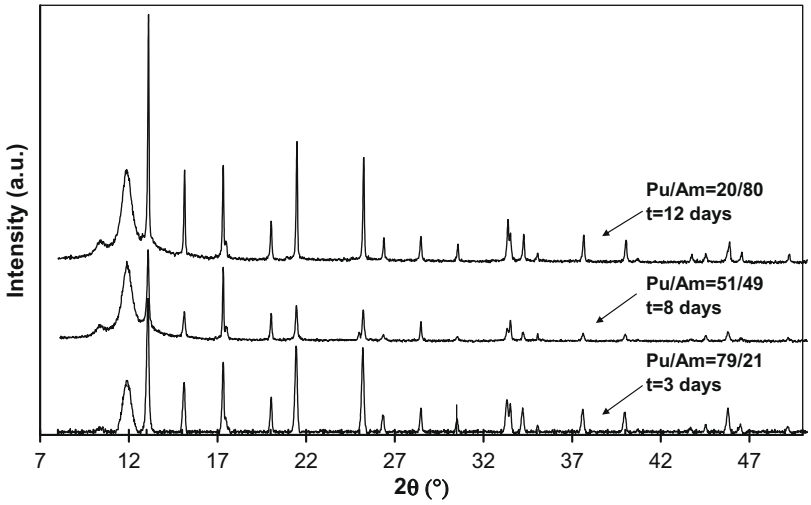

Fig. 2. XRD patterns of the $Pu_{1-x}Am_xO_2$ compounds.

Table 3
Positions and intensities for $Pu_{1-x}Am_xO_2$ (x = 0.2; 0.5; 0.8) compounds.

h k l	$Pu_{0.79}Am_{0.21}O_2$ (3 days after the synthesis)		$Pu_{0.51}Am_{0.49}O_2$ (8 days after the synthesis)		$Pu_{0.20}Am_{0.80}O_2$ (12 days after the synthesis)	
	2θ	Intensity	2θ	Intensity	2θ	Intensity
111	13.073	100	13.089	100	13.102	100
200	15.112	37	15.128	32	15.141	37.5
220	21.441	65	21.454	41	21.176	51.5
311	25.197	63	25.220	37	25.240	45
222	26.338	12	26.359	7.5	26.382	9
400	30.503	9	30.526	4.5	30.555	7.5
331	33.323	*	33.338	*	33.383	*
420	34.209	17	34.232	10	34.265	11.5
422	37.592	17	37.619	8	37.650	11.5
511	39.960	14.5	39.999	8.5	40.031	9.5
440	43.677	3.5	43.757	3	43.750	3.5
533	45.783	*	45.797	*	45.886	*
442	46.481	5	46.482	2.5	46.562	4.5
533	51.105	4	51.137	2	51.169	2
620	49.163	4	49.175	3.5	49.240	3.5
622	51.731	3.5	51.720	2.5	51.843	1.5

* Gold standard peaks overlapping.

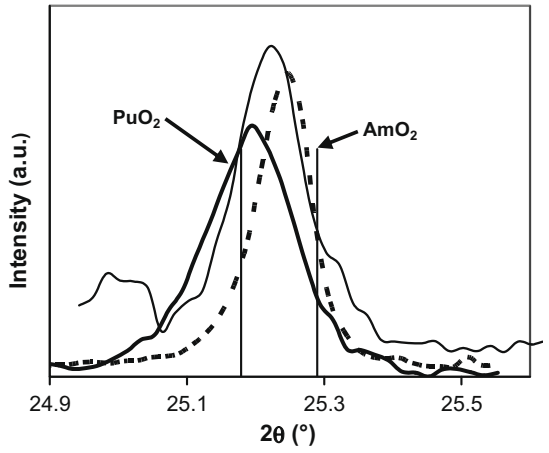

Fig. 3. Comparison between $Pu_{1-x}Am_xO_2$ (x = 0.21: ▬, 0.49: —, 0.8: – –) peaks and AmO_2/PuO_2 peaks.

It can be observed that:

- the lattice parameter expansion rate increases with the Am content as a consequence of the higher cumulative α decay dose;

Table 4
Lattice parameter variation versus time for various AmO_2 and PuO_2 studies.

Compound	a_0 (nm)	$\frac{\Delta a}{a_0}$ (t in days)	References
$^{241}AmO_2$	0.5377	$3.5 \times 10^{-3}\,(1 - e^{-0.042t})$	[5]
$^{241}AmO_2$	0.5377	$2.82 \times 10^{-3}\,(1 - e^{-0.041t})$	[7]
$^{241}AmO_2$	0.53724	$2.39 \times 10^{-3}\,(1 - e^{-13400\lambda t})$	[4]
$^{238(80\%)}PuO_2$	0.53954	$3.2 \times 10^{-3}\,(1 - e^{-0.24t})$	[8]
$^{238(99\%)}PuO_2$	0.53953	$2.83 \times 10^{-3}\,(1 - e^{-10800\lambda t})$	[13]
$^{238(80\%)}PuO_2$	0.53950	$a = 5.441e^{-0.000023t} - 0.027e^{-0.0082t}$	[9]

- the lattice parameter maximum value increases with the Pu content due to the higher PuO_2 lattice parameter;

The influence of the cumulative α decay dose on the lattice parameter variation has also been evaluated. In the case of $Pu_{1-x}Am_xO_2$ mixed oxides, the lattice parameter relative variations were determined using displacements per atom (dpa) because it is directly linked to the number of α decay in the sample and can be used since experiments were carried at room temperature where defects restoration can be neglected. Fig. 5 shows that all experimental data are on the same curve with a maximum of 0.32%. This leads to a global lattice parameter relative variation for

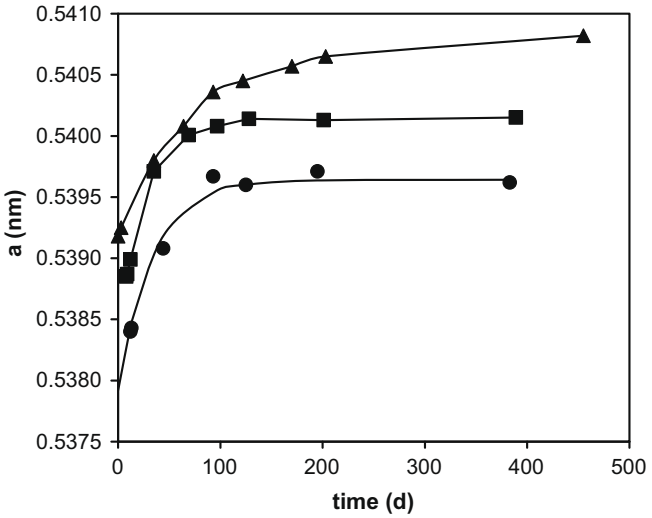

Fig. 4. Lattice parameter variation in $Pu_{1-x}Am_xO_2$ versus time (x = 0.21: ▲; 0.49: ■; 0.8: ●).

Table 5
Initial and maximum values of the lattice parameter in $Pu_{1-x}Am_xO_2$.

Compound	a_0 (nm)	a_{max} (nm)
$Pu_{0.79}Am_{0.21}O_2$	0.5392 ± 0.0001	0.5407 ± 0.0001
$Pu_{0.51}Am_{0.49}O_2$	0.5386 ± 0.0001	0.5401 ± 0.0001
$Pu_{0.20}Am_{0.80}O_2$	0.5379 ± 0.0001	0.5397 ± 0.0001

Table 6
Lattice parameter variation versus time for $Pu_{1-x}Am_xO_2$ (x = 0.2; 0.5; 0.8).

Compound	$\frac{\Delta a}{a_0}$ (t in days)
$Pu_{0.79}Am_{0.21}O_2$	$3.05 \times 10^{-3}\ (1-e^{-0.0127t})$
$Pu_{0.51}Am_{0.49}O_2$	$2.95 \times 10^{-3}\ (1-e^{-0.034t})$
$Pu_{0.20}Am_{0.80}O_2$	$3.20 \times 10^{-3}\ (1-e^{-0.03t})$

$Pu_{1-x}Am_xO_2$ in the range $0.2 < x < 0.8$ which can be expressed as (5):

$$\frac{\Delta a}{a_0} = 0.32 \cdot \left(1 - e^{-80\,\mathrm{dpa}}\right). \quad (5)$$

It is interesting to compare this result to a previous study on $^{239}PuO_2$ [14]. In this latter case, the lattice parameter variation was expressed as (6):

$$\frac{\Delta a}{a_0} = 0.32 \cdot \left(1 - e^{-28.6\,\mathrm{dpa}}\right). \quad (6)$$

In Fig. 5, although the maximum value of the lattice parameter relative variation is the same for PuO_2 and $Pu_{1-x}Am_xO_2$, the expansion rate is higher in the case of the mixed oxides. The physical state of the samples does not explain this difference because in both cases powder was used. The difference comes from powder preparation and more specifically calcination temperature which has an impact on particles size and morphology. For PuO_2, it was carried at high temperature in N_2 while for $Pu_{1-x}Am_xO_2$ the heat treatment was carried in air at a significantly lower temperature. A further study based on the particles morphology would be helpful to understand these different behaviours especially in term of He release.

4. Conclusion

High purity $Pu_{1-x}Am_xO_2$ (x = 0.2; 0.5; 0.8) mixed oxides were synthesized by oxalate co-conversion. For these mixed oxides, no data concerning the structure and self-irradiation phenomenon can be found in the literature. The objective of this work was to study the crystalline structure and the self-irradiation effect in these compounds. The initial lattice parameters and equations which describe the lattice parameter variation were determined for each composition. It was observed a fast lattice parameter expansion rate, followed by a stabilisation at a maximum value. The observations also showed that the initial expansion rate increases with the Am content and the maximum value with the Pu content. Finally, it was found that, for the three compositions, the lattice parameter relative variations are the same.

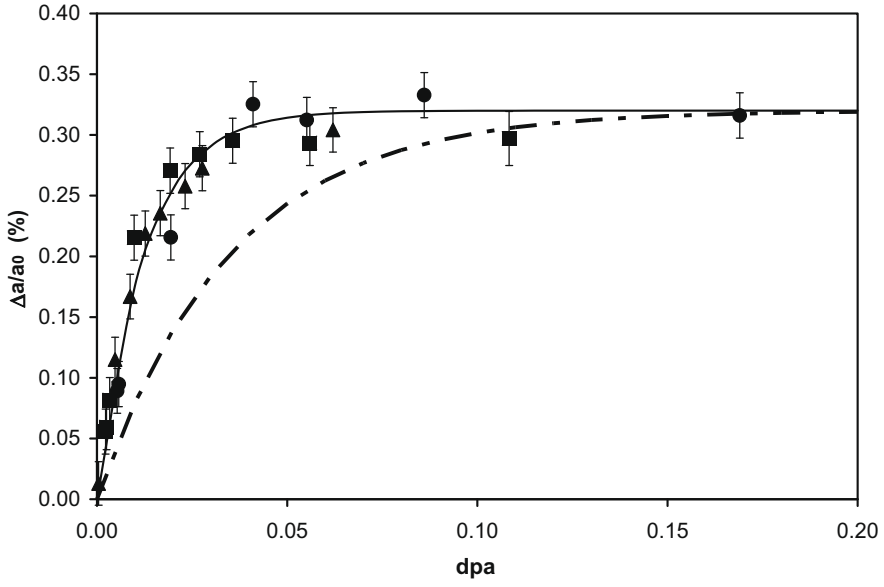

Fig. 5. Global lattice parameter variation in $Pu_{1-x}Am_xO_2$ versus dpa, (x = 0.21: ▲; 0.49: ■; 0.8: ●), ▬: this study; - -:[14].

Acknowledgments

The authors express their gratitude to all the scientists and Institutes involved in EUROTRANS project and to the European Commission for the financial support under the FI6 W-CT-2004 contract.

References

[1] F.W. Clinard Jr., L.W. Hobbs, J. Nucl. Mater. 105 (1982) 248.
[2] S. Casalta, Hj. Matzke, C. Prunier, Global (1995) 1667.
[3] T.D. Chikalla, R.E. Skavdahl, Rapport BNWL-150, BNWL-198, 1965.
[4] C. Hurtgen et al., Inorg. Nucl. Chem. Lett. 13 (1977) 179.
[5] C. Keller, The solid-state chemistry of americium oxides, in: Gould, A.F., (Eds.), Advances in Chemistry Series, vol. 71, 1967, (Chapter 17).
[6] K. Mendelssohn, K. King, J. Lee, in: A.E. Kay, M.B. Waldron, (Eds.), Plutonium, 1965, p. 189.
[7] T.D. Chikalla, L. Eyring, J. Inorg. Nucl. Chem. 30 (1968) 133.
[8] R.P. Turcotte, T.D. Chikalla, Radiat. Eff. 19 (1973) 99.
[9] R.B. Roof, Adv. X-ray Anal. 16 (1973) 396.
[10] W.J. Nellis, Inorg. Nucl. Chem. Lett. 13 (1977) 393.
[11] J. Fuger, Inorg. Chem. 7 (1975). Chapter 5.
[12] P.T. Elton, Alpha particle damage in oxide nuclear, Rapport SRD R405, 1987.
[13] M. Noé, J. Fuger, Inorg. Nucl. Chem. Lett. 10 (1973) 7.
[14] D.B. Mc Whan, B.B. Cunningham, J.C. Wallman, J. Inorg. Nucl. Chem. 24 (1962) 1025.